Chip-based microtrap arrays for cold polar molecules

Shunyong Hou, Bin Wei, Lianzhong Deng, and Jianping Yin*
State Key Laboratory of Precision Spectroscopy, East China Normal University, Shanghai 200062, China
(Received 13 August 2017; published 20 December 2017)

Compared to the atomic chip, which has been a powerful platform to perform an astonishing range of applications from rapid Bose-Einstein condensate (BEC) production to the atomic clock, the molecular chip is only in its infant stages. Recently a one-dimensional electric lattice was demonstrated to trap polar molecules on a chip. This excellent work opens up the way to building a molecular chip laboratory. Here we propose a two-dimensional (2D) electric lattice on a chip with concise and robust structure, which is formed by arrays of squared gold wires. Arrays of microtraps that originate in the microsize electrodes offer a steep gradient and thus allow for confining both light and heavy polar molecules. Theoretical analysis and numerical calculations are performed using two types of sample molecules, ND_3 and SrF, to justify the possibility of our proposal. The height of the minima of the potential wells is about 10 μm above the surface of the chip and can be easily adjusted in a wide range by changing the voltages applied on the electrodes. These microtraps offer intriguing perspectives for investigating cold molecules in periodic potentials, such as quantum computing science, low-dimensional physics, and some other possible applications amenable to magnetic or optical lattice. The 2D adjustable electric lattice is expected to act as a building block for a future gas-phase molecular chip laboratory.

DOI: 10.1103/PhysRevA.96.063416

I. INTRODUCTION

Atomic chips and lattices are two powerful tools for manipulating and cooling neutral atoms. The atomic chip is now reaching maturity [1] as a powerful art with many applications in modern science ranging from fast Bose-Einstein condensate (BEC) generation [2] to precision measurements [3]. However, the molecular chip is only in its infant stages, in part because molecules have much richer internal states which are immune to effective cooling and manipulating. Fortunately, many methods have been demonstrated over the years to produce molecular samples in both cold (<1 K) [4–8] and ultracold (<1 mK) [9–13] temperature regions. Especially, the recently realized methods of laser cooling for molecules [14–20], which have been the workhorse in the field of ultracold atoms, bridge the two regions of cold and ultracold temperature of the molecules. These (ultra-) cold molecules offer more possibilities for engineering a gas-phase chip laboratory, which in fact is a long-standing goal in atomic, molecular, and optical physics as well as cold chemistry.

Lattices, formed by electric fields, magnetic fields, or laser light, have attracted great interest because they offer opportunities to study particles in an ordered structure and allow for spatial and temporal control of particles at a high level. These features make it a good candidate in applications ranging from quantum simulation to atomic clocks. Currently one-, two-, and three-dimensional (1D, 2D, and 3D) optical [21–25], magnetic [26–29], and magneto-optical [29–31]) lattices have already been demonstrated or proposed. Recently Meijer's group demonstrated a 1D electric lattice (a Stark decelerator on a chip) that can trap polar molecules on a chip [32,33]. This demonstration constitutes an important step towards a gas-phase molecular laboratory on a chip. Recently, they demonstrated a series of works based on the 1D lattice, including manipulating the internal degrees of freedom [34,35] and measuring the temperature of the trapped molecules [36]. Recently Merkt's group demonstrated a 1D lattice for Rydberg atoms on a printed circuit board [37].

In this paper we propose a 2D electric lattice on a chip for cold polar molecules. The electric lattice can offer a large force and allows for trapping both light and heavy polar molecules. The height of the minima of the potential wells can be adjusted in a wide range by changing the voltages applied on the electrodes. This 2D adjustable electric lattice may provide opportunities for investigating many issues, such as the study of the interaction between polar molecules or molecule-surface interaction, novel quantum mechanical collision, quantum information science, and so on. We note that most recently a simple and versatile method, optoelectrical Sisyphus cooling in a microstructured electric trap, to produce submillikelvin polar molecular samples has been demonstrated [38], with a four-order-of-magnitude increase of phase space density. This gives us some inspiration that our 2D electric lattice might also be possible to prepare arrays of ultracold molecular samples on a chip with the help of optoelectrical Sisyphus cooling. In the following sections, we will present the design of the 2D electric lattice. Following that, the theoretical analyses of the lattice and trajectory calculations using two types of molecules, ND_3 and SrF, are given to justify the possibility of our scheme, which is followed by some applications and conclusions.

II. DESIGN

Figure 1(a) depicts a typical scheme preparing and loading polar cold molecules onto a molecular chip. A supersonic molecular beam is slowed down by a Stark decelerator and then loaded onto a chip, where our designed 2D electrostatic lattice is deposited. The 2D electrostatic lattice consists of arrays of 1-μm-high gold electrodes patterned with concentric squares, as shown in Fig. 1(b). Figure 1(c) depicts the expanded view of the local electrostatic lattice. As can be seen one site is composed of three concentric square electrodes. The innermost

*jpyin@phy.ecnu.edu.cn

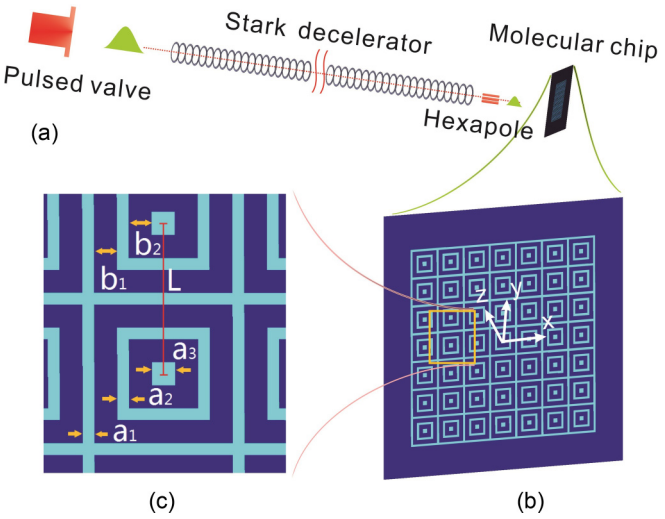

FIG. 1. (a) illustration of producing and loading cold polar molecules into an electrostatic lattice on a chip; (b) pattern of our designed 2D electrostatic lattice as well as the coordinates used in the text; (c) expanded view of the local 2D electrostatic lattice, together with the geometric parameters of the electrodes.

electrode is a small square with a side of length a_3. The middle and the outermost electrodes are square wires, which have a width of a_2 and a_1, respectively. All outermost electrodes are connected together and are shared with the neighbor sites, on which the voltage applied is U_2. The middle (innermost) electrodes are connected together with thin wires (not shown) under the chip and taken with a voltage of U_1 (U_0). The gap between the innermost and the middle electrodes is b_2, while the spacing of the outermost and the middle electrodes is b_1. The periodicity of the lattice, i.e., the center-to-center distance of the adjacent sites, is L. In the following test the parameters are set as follows: $a_1 = a_2 = 5\,\mu$m, $a_3 = 10\,\mu$m, and $b_1 = b_2 = 10\,\mu$m. As a result the periodicity of the lattice L is 65 μm. The coordinate system is also shown in Fig. 1(b), in which the z direction is normal to the molecule chip surface and oriented in the direction opposite to the molecular beam.

III. THEORETICAL ANALYSIS AND NUMERICAL CALCULATIONS

In a charge-free region of space the electric potential $\Phi(x,y,z)$ must be a solution to Laplace's equation. The electric potential $\Phi(x,y,z)$ of our designed 2D electric lattice is given by

$$\Phi(x,y,z) = \sum_{m,n=0}^{\infty} A_{mn} \exp[-z\sqrt{(mk_x x)^2 + (nk_y y)^2}] \times [\cos(mk_x x)\cos(nk_y y)], \quad (1)$$

where $k_x = k_y = 2\pi/L$, and L is the periodicity of the potential. The coefficients A_{mn} are determined by comparing the numerically calculated fields along lines in the x (y) direction, using a method similar to Ref. [39]. We choose $m = n = 0, 1, 2, 3$ to create quadrupole potentials in the transverse directions. As long as the electric potential is constrained, the electric field strength is given by

$$|\vec{E}| = \sqrt{\left(\frac{\partial\Phi}{\partial x}\right)^2 + \left(\frac{\partial\Phi}{\partial y}\right)^2 + \left(\frac{\partial\Phi}{\partial z}\right)^2}. \quad (2)$$

Then the force between the polar molecules and the fields can be derived as in the following:

$$F_x = -\left(\frac{1}{|\vec{E}|}\frac{dW}{d|\vec{E}|}\right)\left(\frac{\partial^2\Phi}{\partial x^2}\frac{\partial\Phi}{\partial x} + \frac{\partial^2\Phi}{\partial x\partial y}\frac{\partial\Phi}{\partial y} + \frac{\partial^2\Phi}{\partial y\partial z}\frac{\partial\Phi}{\partial z}\right), \quad (3a)$$

$$F_y = -\left(\frac{1}{|\vec{E}|}\frac{dW}{d|\vec{E}|}\right)\left(\frac{\partial^2\Phi}{\partial x\partial y}\frac{\partial\Phi}{\partial x} + \frac{\partial^2\Phi}{\partial y^2}\frac{\partial\Phi}{\partial y} + \frac{\partial^2\Phi}{\partial y\partial z}\frac{\partial\Phi}{\partial z}\right), \quad (3b)$$

$$F_z = -\left(\frac{1}{|\vec{E}|}\frac{dW}{d|\vec{E}|}\right)\left(\frac{\partial^2\Phi}{\partial x\partial z}\frac{\partial\Phi}{\partial x} + \frac{\partial^2\Phi}{\partial y\partial z}\frac{\partial\Phi}{\partial y} - \left(\frac{\partial^2\Phi}{\partial x^2} + \frac{\partial^2\Phi}{\partial y^2}\right)\frac{\partial\Phi}{\partial z}\right), \quad (3c)$$

where W is the Stark potential. When $U_1 = -U_2 = 90$ V and U_0 is grounded, the electric fields above the chip are calculated using Eqs. (1) and (2), as shown in Fig. 2. Figures 2(a) and 2(b) reflect the electric field distributions in the x-y plane

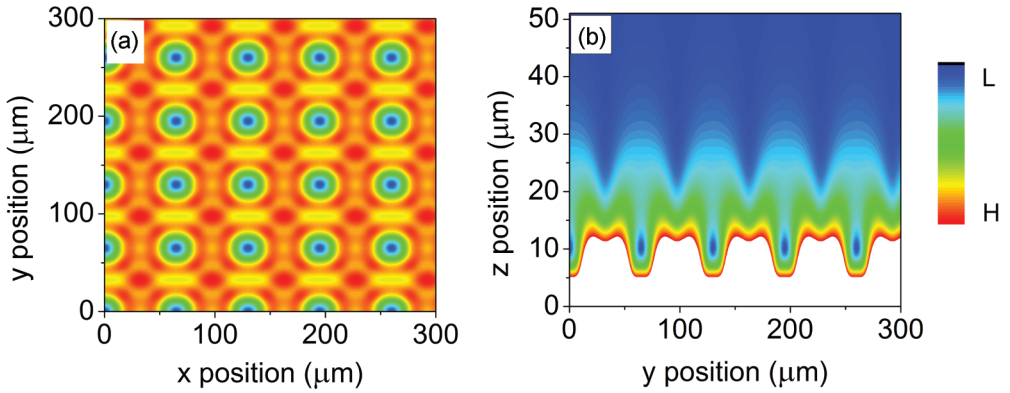

FIG. 2. Electric field distribution of the 2D lattice in the x-y plane (a) and in the y-z plane (b) through the minima of the potential wells. The height of the minima of the potential is about 10 μm (in the z direction) above the surface of the chip. Color bar labels H and L mean high and low electric field, respectively.

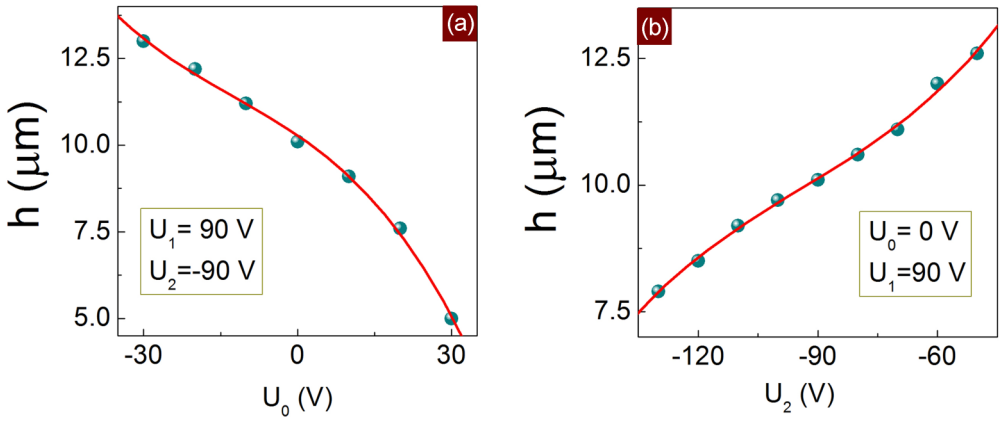

FIG. 3. The height of the minima of the potential wells as a function of the voltages U_0 (a) and U_2 (b). When the value of one voltage applied on the electrodes is changed, the other two voltages are fixed in both (a) and (b). The points are obtained from numerical calculations and the lines are fitting results.

and in the y-z plane through the minima of the potential wells, respectively. As can be seen from this figure, arrays of microtraps (i.e., 2D electric lattice) for polar molecules in low-field seeking states can be formed above the chip. It is worth nothing that the height of the minima of the potentials from the surface of the substrate remains constant regardless of the values of U_1 and U_2, provided that $U_1 = -U_2$. However, the height of the minima of the potential wells can be changed by adjusting the voltage difference of the neighboring electrodes. Figure 3 shows two means to controlling the height (h) of the minima. In the first case, U_1 and U_2 are respectively set to constant values of 90 and -90 V, and the value of U_0 is tuned from -30 to 30 V, resulting in the decreasing of h from 13.0 to 5.0 μm, as shown in Fig. 3(a). In the second case, U_0 is grounded and U_1 is taken with 90 V; the voltage U_2 is changed from -130 to -50 V, and as a result h is correspondingly changed from 7.9 to 12.6 μm. Of course, the height of the minima can also be adjusted in a wider range by simultaneously changing both values of U_0 and U_2. For instance, with $U_0 = -30$ V, $U_1 = 90$ V, and $U_2 = -60$ V, $h = 15.0\,\mu$m is obtained.

Our 2D electrostatic lattice can produce a steep gradient in all three directions that allows for confining not only light polar molecules but also some heavy ones. To show the performance of our scheme, two species—ND_3 (in the $|J,KM\rangle = |1,-1\rangle$ state) and SrF (in the $|N,N_M\rangle = |1,0\rangle$ state)—are used to carry out 3D numerical calculations. Losses caused by background collision and surface-induced heating are ignored in our simulation since current vacuum technology and cooling technology permit greatly reducing these losses [40]. Nonadiabatic transition loss, which can be suppressed by using an offset magnetic field [41], is also not considered in our calculation. The position and velocity distributions of the initial molecular beam are flat in all directions with the six-dimensional (6D) emittance [100 μm × 1.5 m/s] × [150 μm × 1.5 m/s] × [150 μm × 1.5 m/s] (in z, x, and y axis, respectively). The beam contains 1 000 000 molecules with initial distribution centered at $y = 0\,\mu$m, $v_y = 0$ m/s, $x = 0\,\mu$m, $v_x = 0$ m/s, $z = 3$ mm, $v_z = 12$ m/s (ND_3), or $v_z = 5$ m/s (SrF). The above parameters of the molecular beam are chosen by referring to some recent experimental results [42,43]. U_0 is grounded and the voltages U_1, U_2 applied on the electrodes are 90 and -90 V, respectively.

The trajectory simulation starts from the exit of the hexapole downstream of the Stark decelerator, about 3 mm away from the surface of the chip. In the simulation we employ a so-called "synchronous molecule" to create the time sequence of operations. The synchronous molecule is virtual and is always in sync with operations of the external fields. Figure 4(a) shows the loading process that covers three steps: First, the synchronous molecule flies from the exit of the hexapole to position A, about 20 μm above the surface of the chip, and is further decelerated by the electrostatic fields produced by the 2D lattice. The voltages applied on the lattice will be switched off immediately when the synchronous molecule reaches position A. At the second step the synchronous molecule freely flies from position A to B, and then the electric fields switch on again. At the third step the synchronous molecule will be brought to a standstill at position C by the electric fields and is finally confined by the lattice. In fact, the nonsynchronous molecules around the synchronous molecule can also be manipulated, and only those in the phase space acceptance of the potential wells can be confined by the traps. The orange line in Fig. 4(b) shows a typical longitudinal acceptance of an individual trap in the lattice. The velocity of the synchronous molecule in the following discussion is set to the central velocity of the packets, and thus the central part of the packets can be trapped and other molecules are lost. The electric fields at the vicinity of the chip and the force felt by each molecule at any location are calculated using Eqs. (1)–(3). The calculated results of the trapping process are shown in Fig. 4(c), where the black line shows the time dependence of the molecular density of the trapped ND_3 molecules. It is clear that the molecules can be stably confined in the lattice. The Stark shift of ND_3 close to the center of the trap is quadratic and thus the restoring force is linearly proportional to the displacement. The trap frequency can be estimated by taking the potential well as a harmonic trap. Thus the expression of the potential well is given by $U_z = k_z z^2/2$, where $k_z = m\omega_z^2$. This yields the longitudinal trap frequency $f_z = \omega_z/2\pi = 348$ kHz, matching with the fitting result, $f_z = 340$ kHz, obtained by fitting the oscillation of trapped ND_3 in the z direction, as shown in the

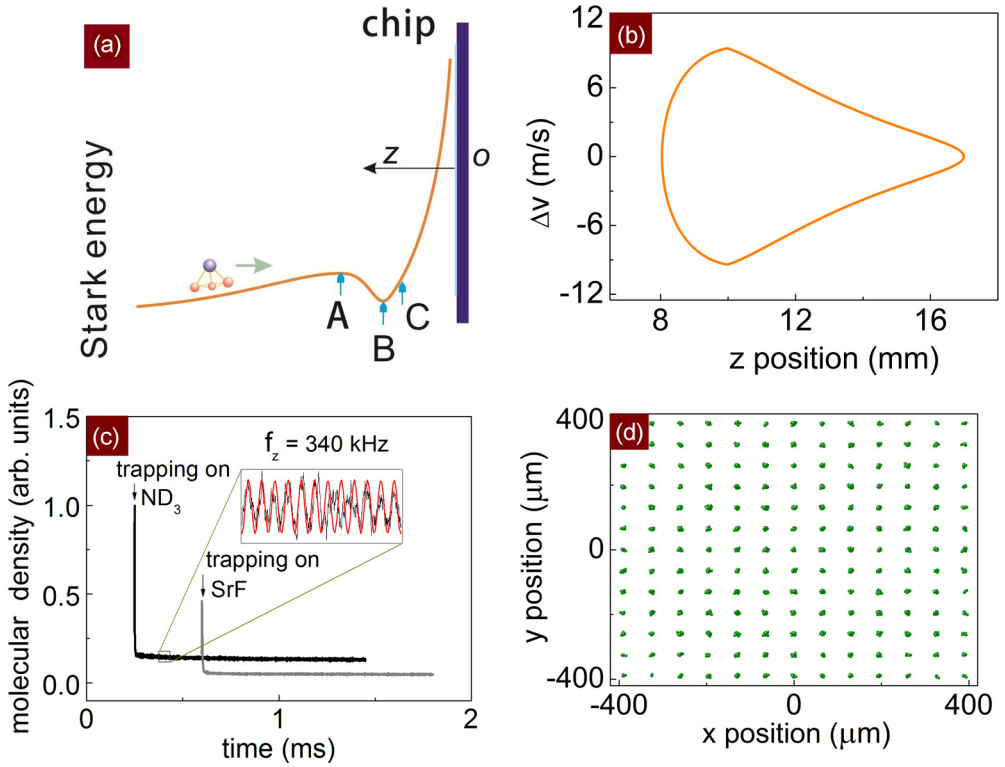

FIG. 4. (a) Loading process of cold molecules into the 2D electric lattice. The solid line indicates the Stark energy of the polar molecules along the z axis near the surface of the chip. (b) A typical longitudinal acceptance of an individual trap of the electric lattice for ND_3 molecule. (c) Time dependence of molecular density of ND_3 (black line) and SrF (gray line) in the lattice. The expanded view shows the oscillation of trapped ND_3 in the z direction, where the red line is the fitting result that results from $f_z = 340$ kHz. (d) The spatial distribution of the ND_3 samples in the 2D lattice.

inset in Fig. 4(c). It is usually more difficult to tame heavy polar molecules (>100 amu) because they have more kinetic energy for a given velocity, and because their Stark curve of the rotational energy levels easily turns down at high electric fields. The SrF molecule in the $|N, N_M\rangle = |1,0\rangle$ state is always low-field seeking [44] in our designed electric lattice. The results of the trajectory calculation of loading and trapping SrF molecules are shown in Fig. 4(c). It is clear that the molecular density of SrF can also be stably confined in the lattice, albeit about three time less than ND_3 molecules. It shows that heavy polar molecules are also amenable to our designed 2D electric lattice, which offers more possibilities for basic research and application work. Figure 4(d) indicates the spatial distribution of the molecular sample confined by the 2D lattice.

IV. ADIABATIC COOLING AND DISCUSSION

In this section we will discuss some possible applications of our 2D electric lattice. Recently quantum computing has attracted great interest and a variety of quantum computing schemes with polar molecules have been suggested [45–49]. Our controllable 2D electric lattice on a chip enables stably confining various polar molecules and is conveniently combined with laser light or microwaves to form a hybrid system that may find applications in quantum information science. It is also convenient to study the reflection of a laser beam (such as Bragg scattering) from the polar molecules ordered by the 2D electric lattice. Our designed 2D lattice can be used to investigate molecule-surface interaction or interaction between polar molecules since the heights of the potential wells are easily changed by tuning the voltages applied on the lattice. It might also be possible to use the 2D electric lattice to prepare arrays of small (ultra-) cold molecular samples and even molecular Bose-Einstein condensates using the methods of adiabatic cooling, Sisyphus cooling, or evaporative cooling, which have been exploited for atoms [50–51] or molecules [16] in a single chip-based trap.

Adiabatic cooling of molecules trapped in a 1D electric lattice on a chip was studied [36,52]. In the following discussion, we will give examples of adiabatic and nonadiabatic cooling of trapped molecules in our 2D electric lattice using the method of Monte Carlo simulation. The initial beam contains 5 000 000 ND_3 molecules with initial distribution centered at $z = 10\,\mu$m, $v_z = 0$ m/s, $y = 0\,\mu$m, $v_y = 0$ m/s, and $x = 0\,\mu$m, $v_x = 0$ m/s. The position and velocity distributions of the initial molecular beam are flat in all directions with the 6D emittance $[10\,\mu\text{m} \times 12\,\text{m/s}] \times [500\,\mu\text{m} \times 15\,\text{m/s}] \times [500\,\mu\text{m} \times 15\,\text{m/s}]$ (in the z, x, and y directions, respectively), which are larger than the acceptance of individual sites of the lattice. In the adiabatic process, the voltages applied on the 2D lattice ($|U_{1,2}|$) are slowly reduced from 100 V to a lower value in 500 μs, and then kept at the lower voltage for another 500 μs. Subsequently the voltages are slowly increased back to 100 V in 500 μs and kept for 300 μs. U_0 is always grounded in the adiabatic process. The time sequence is shown on the left of Fig. 5(a).

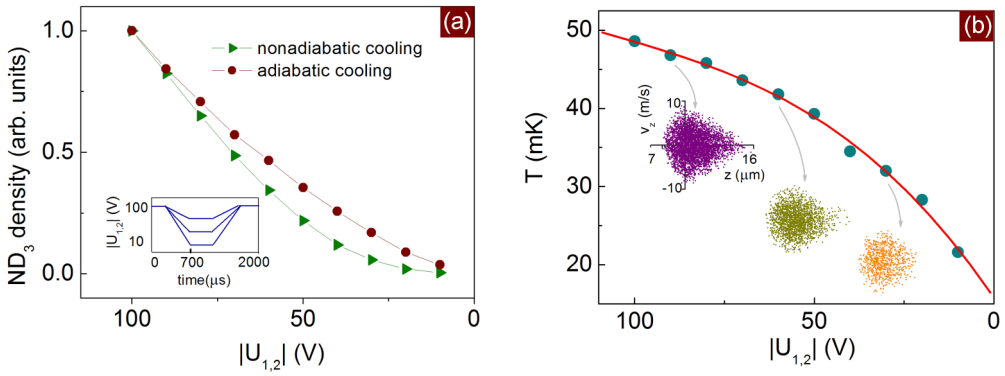

FIG. 5. (a) Simulated results of trapped ND_3 density as a function of voltages $|U_{1,2}|$. The dots and triangles respectively represent two operation manners that slowly (adiabatic cooling) or abruptly (nonadiabatic cooling) decrease the voltage of $|U_{1,2}|$, where the amplitudes of U_1 and U_2 are always equal but differ in polarity in the cooling processes. The left inset indicates the time sequence for the adiabatic cooling. (b) The temperature of trapped ND_3 molecules as a function of $|U_{1,2}|$ in the adiabatic cooling process, together with the phase space distributions of ND_3 in the z direction at different values of $|U_{1,2}|$, as shown on the left.

Lowering the voltages of the lattice leads to the hottest molecules to escape from the traps and allows for adiabatic cooling of the molecules. Note that the ramping time should be sufficiently long for molecules to adiabatically follow the change in potential: $d\omega/dt \ll \omega^2$ [53], i.e., $dT/dt \ll 1$. As mentioned before, the trap frequency of our lattice can be estimated by approximating the central part ($10\,\mu$m) of the trapping potential, where most molecules are situated, with a harmonic one expressed as $U = k(x^2 + y^2 + z^2)/2$. The trap frequency $f = \omega/2\pi = \sqrt{k/m}/2\pi$, where m is the mass of the molecules. This leads to the trap frequency $f = 370\,$kHz (or 120 kHz) at $U_{1,2} = 100\,$V (or 10 V). As a result, the trap period is varied from 3 to 7 μs in the adiabatic process with lowering the voltages $|U_{1,2}|$ from 100 to 10 V. Taking $\Delta T = 7\,\mu$s, for instance, the ramping time $\Delta t = 500$, and thus $\Delta T/\Delta t = 7\,\mu\text{s}/500\,\mu\text{s} = 0.014$, which satisfies the adiabatic condition. In other words, the ramping time of 500 μs is sufficiently long for molecules to adiabatically follow the change in potential even when the voltages $|U_{1,2}|$ are reduced to the lowest value of 10 V. The dots in Fig. 5(a) are the calculated results of adiabatic cooling, where the depths of the traps are correspondingly decreased from 220 to 22 mK with $|U_{1,2}|$ reducing from 100 to 10 V. The time sequence for the nonadiabatic cooling is similar to the adiabatic case, but the voltages ramp abruptly down or up in order to avoid adiabatic cooling of the molecules. The calculated results of nonadiabatic cooling are also presented in Fig. 5(a) in the form of triangles. Compared to the adiabatic cooling, the number density of the trapped molecules in the nonadiabatic case is decreased first rapidly and then slowly along with lowering the voltages of $|U_{1,2}|$.The temperature of the molecular samples in the lattice is reduced along with the lowering voltages of $|U_{1,2}|$ in the adiabatic cooling process, as shown in Fig. 5(b). The temperature T is defined by $(3/2)k_BT = (1/2)k_BT_L + k_BT_T$ [54], where T_L and T_T are the corresponding longitudinal and transverse temperatures of the molecular packets and are given by $T_{x,y,z} = m\Delta v_{x,y,z}^2/8\ln 2k_B$ [55], with m being the mass, $\Delta v_{x,y,z}$ the velocity spread (full width at half maximum), and k_B the Boltzmann constant. When the initial voltage of $|U_{1,2}|$ is decreased from 100 to 10 V, the temperature of the molecular samples is correspondingly decreased from 49 mK to around 21 mK. It means a reduction in temperature to about 40%. The insets on the left of Fig. 5(b) indicate the phase space distributions of trapped ND_3 in the z direction at three selected values of $|U_{1,2}|$ in the adiabatic cooling process. It is clear that the volume of the molecules in phase space becomes smaller with lowering the voltages of $|U_{1,2}|$.

V. CONCLUSIONS

We have presented a promising design of the scheme of a 2D electric lattice on a chip that has a very concise and robust structure. The height of the minima of the potential wells is about 10 μm above the chip, which can easily be adjusted in a wide range (5.0–15.0 μm) by changing the voltages applied on the electrodes. Two types of sample molecules, ND_3 (in the $|J,KM\rangle = |1,-1\rangle$ state) and SrF (in the $|N,N_M\rangle = |1,0\rangle$ state) are used in numerical calculations to justify the possibility of our scheme in confining both light and heavy polar molecules. In addition, adiabatic and nonadiabatic cooling trapped ND_3 molecules in the 2D lattice are also studied using the method of Monte Carlo simulation.

The high level of spatial control of local fields offered by the molecular chip makes it an ideal tool for supporting a variety of applications as well as basic research such as quantum computing, molecule-surface interaction, low-dimensional physics, and more. Besides, our design of a 2D electric lattice is scalable and flexible to expand to various geometry patterns to produce other more complex potentials like honeycombed and disordered structures, and it offers opportunities to study particles in a (dis-) ordered structure. In summary, it may be possible for our proposed controllable 2D electric lattice to act as a building block for a future molecular chip laboratory.

ACKNOWLEDGMENTS

We gratefully acknowledge fruitful discussions with Dr. Tao Yang. This work is supported by the National Nature Science Foundation of China (Grants No. 91536218, No. 11034002, No. 11274114, and No.11504112) and the National Key Basic Research and Development Program of China (Grant No. 2011CB921602).

[1] M. Keil, O. Amit, S. Zhou, D. Groswasser, Y. Japha, and R. Folman, J. Mod. Opt. **63**, 1840 (2016).

[2] W. Hänsel, P. Hommelhoff, T. W. Hänsch, and J. Reichel, Nature **413**, 498 (2001).

[3] S. Abend, M. Gebbe, M. Gersemann, H. Ahlers, H. Müntinga, E. Giese, N. Gaaloul, C. Schubert, C. Lämmerzahl, W. Ertmer, W. P. Schleich, and E. M. Rasel, Phys. Rev. Lett. **117**, 203003 (2016).

[4] J. D. Weinstein, R. deCarvalho, T. Guillet, B. Friedrich, and J. M. Doyle, Nature **395**, 148 (1998).

[5] L. D. van Buuren, C. Sommer, M. Motsch, S. Pohle, M. Schenk, J. Bayerl, P. W. H. Pinkse, and G. Rempe, Phys. Rev. Lett. **102**, 033001 (2009).

[6] H. L. Bethlem, G. Berden, and G. Meijer, Phys. Rev. Lett. **83**, 1558 (1999).

[7] N. Vanhaecke, U. Meier, M. Andrist, B. H. Meier, and F. Merkt, Phys. Rev. A **75**, 031402 (2007).

[8] R. Fulton, A. I. Bishop, and P. F. Barker, Phys. Rev. Lett. **93**, 243004 (2004).

[9] J. D. Miller, R. A. Cline, and D. J. Heinzen, Phys. Rev. Lett. **71**, 2204 (1993).

[10] P. D. Lett, K. Helmerson, W. D. Phillips, L. P. Ratliff, S. L. Rolston, and M. E. Wagshul, Phys. Rev. Lett. **71**, 2200 (1993).

[11] S. Jochim, M. Bartenstein, A. Altmeyer, G. Hendl, S. Riedl, C. Chin, J. H. Denschlag, and R. Grimm, Science **302**, 2101 (2003).

[12] C. A. Regal, C. Ticknor, J. L. Bohn, and D. S. Jin, Nature **424**, 47 (2003).

[13] M. W. Zwierlein, C. A. Stan, C. H. Schunck, S. M. F. Raupach, S. Gupta, Z. Hadzibabic, and W. Ketterle, Phys. Rev. Lett. **91**, 250401 (2003).

[14] E. S. Shuman, J. F. Barry, D. R. Glenn, and D. DeMille, Phys. Rev. Lett. **103**, 223001 (2009).

[15] E. S. Shuman, J. F. Barry, and D. DeMille, Nature **467**, 820 (2010).

[16] M. Zeppenfeld, B. G. U. Englert, R. Glöckner, A. Prehn, M. Mielenz, C. Sommer, L. D. van Buuren, M. Motsch, and G. Rempe, Nature **491**, 570 (2012).

[17] M. T. Hummon, M. Yeo, B. K. Stuhl, A. L. Collopy, Y. Xia, and J. Ye, Phys. Rev. Lett. **110**, 143001 (2013).

[18] V. Zhelyazkova, A. Cournol, T. E. Wall, A. Matsushima, J. J. Hudson, E. A. Hinds, M. R. Tarbutt, and B. E. Sauer, Phys. Rev. A **89**, 053416 (2014).

[19] J. F. Barry, D. J. McCarron, E. B. Norrgard, M. H. Steinecker, and D. DeMille, Nature **512**, 286 (2014).

[20] I. Kozyryev, L. Baum, K. Matsuda, B. Hemmerling, and J. M. Doyle, J. Phys. B: At., Mol. Opt. Phys. **49**, 134002 (2016).

[21] P. Verkerk, B. Lounis, C. Salomon, C. Cohen-Tannoudji, J.-Y. Courtois, and G. Grynberg, Phys. Rev. Lett. **68**, 3861 (1992).

[22] P. S. Jessen, C. Gerz, P. D. Lett, W. D. Phillips, S. L. Rolston, R. J. C. Spreeuw, and C. I. Westbrook, Phys. Rev. Lett. **69**, 49 (1992).

[23] A. Hemmerich and T. W. Hänsch, Phys. Rev. Lett. **70**, 410 (1993).

[24] A. Hemmerich, C. Zimmermann, and T. W. Hänsch, Europhys. Lett. **22**, 89 (1993).

[25] G. Grynberg, B. Lounis, P. Verkerk, J.-Y. Courtois, and C. Salomon, Phys. Rev. Lett. **70**, 2249 (1993).

[26] A. Günther, S. Kraft, M. Kemmler, D. Koelle, R. Kleiner, C. Zimmermann, and J. Fortágh, Phys. Rev. Lett. **95**, 170405 (2005).

[27] R. Gerritsma, S. Whitlock, T. Fernholz, H. Schlatter, J. A. Luigjes, J.-U. Thiele, J. B. Goedkoop, and R. J. C. Spreeuw, Phys. Rev. A **76**, 033408 (2007).

[28] J. P. Yin, W. J. Gao, J. J. Hu, and N. C. Liu, Chin. Phys. Lett. **19**, 327 (2002).

[29] J. P. Yin, W. J. Gao, J. J. Hu, and Y. Q Wang, Opt. Commun. **206**, 99 (2002).

[30] A. Grabowskia and T. Pfau, Eur. Phys. J. D **22**, 347 (2003).

[31] S. Pollock, J. P. Cotter, A. Laliotis, and E. A. Hinds, Opt. Express **17**, 14109 (2009).

[32] S. A. Meek, H. L. Bethlem, H. Conrad, and G. Meijer, Phys. Rev. Lett. **100**, 153003 (2008).

[33] S. A. Meek, H. Conrad, and G. Meijer, Science **324**, 1699 (2009).

[34] G. Santambrogio, S. A. Meek, M. J. Abel, L. M. Duffy, and G. Meijer, Chem. Phys. Chem. **12**, 1799 (2011).

[35] M. J. Abel, S. Marx, G. Meijer, and G. Santambrogio, Mol. Phys. **110**, 1829 (2012).

[36] S. Marx, D. Adu Smith, G. Insero, S. A. Meek, B. G. Sartakov, G. Meijer, and G. Santambrogio, Phys. Rev. A **92**, 063408 (2015).

[37] S. D. Hogan, P. Allmendinger, H. Saßmannshausen, H. Schmutz, and F. Merkt, Phys. Rev. Lett. **108**, 063008 (2012).

[38] A. Prehn, M. Ibrügger, R. Glöckner, G. Rempe, and M. Zeppenfeld, Phys. Rev. Lett. **116**, 063005 (2016).

[39] S. A. Meek, Ph.D. thesis, Freie Universität, 2010.

[40] S. Y. Buhmann, M. R. Tarbutt, S. Scheel, and E. A. Hinds, Phys. Rev. A **78**, 052901 (2008).

[41] S. A. Meek, G. Santambrogio, B. G. Sartakov, H. Conrad, and G. Meijer, Phys. Rev. A **83**, 033413 (2011).

[42] F. M. H. Crompvoets, R. T. Jongma, H. L. Bethlem, A. J. A. van Roij, and G. Meijer, Phys. Rev. Lett. **89**, 093004 (2002).

[43] S. Y. T. van de Meerakker, H. L. Bethlem, and G. Meijer, Nat. Phys. **4**, 595 (2008).

[44] S. Hou, B. Wei, L. Deng, and J. Yin, Sci. Rep. **6**, 32663 (2016).

[45] D. DeMille, Phys. Rev. Lett. **88**, 067901 (2002).

[46] S. F. Yelin, K. Kirby, and R. Côté, Phys. Rev. A **74**, 050301 (2006).

[47] A. André, D. Demille, J. M. Doyle, M. D. Lukin, S. E. Maxwell, P. Rabl, R. J.Schoelkopf, and P. Zoller, Nat. Phys. **2**, 636 (2006).

[48] E. Kuznetsova, R. Côté, K. Kirby, and S. F. Yelin, Phys. Rev. A **78**, 012313 (2008).

[49] P. Rabl, D. DeMille, J. M. Doyle, M. D. Lukin, R. J. Schoelkopf, and P. Zoller, Phys. Rev. Lett. **97**, 033003 (2006).

[50] A. Kastberg, W. D. Phillips, S. L. Rolston, R. J. C. Spreeuw, and P. S. Jessen, Phys. Rev. Lett. **74**, 1542 (1995).

[51] J. Märkle, A. J. Allen, P. Federsel, B. Jetter, A. Günther, J. Fortágh, N. P. Proukakis, and T. E. Judd, Phys. Rev. A **90**, 023614 (2014).

[52] B. G. U. Englert, M. Mielenz, C. Sommer, J. Bayerl, M. Motsch, P. W. H. Pinkse, G. Rempe, and M. Zeppenfeld, Phys. Rev. Lett. **107**, 263003 (2011).

[53] L. D. Landau and E. M. Lifshitz, *Mechanics*, 3rd ed. (Butterworth-Heinemann, Oxford, 1993), Vol. 1.

[54] *Atomic and Molecular Beam Methods*, edited by G. Scoles (Oxford University Press, New York, 1986), p. 27.

[55] M. Gupta and D. Herschbach, J. Phys. Chem. A **103**, 10670 (1999).